Gap electroacoustic waves in *PT*-symmetric piezoelectric heterostructure near the exceptional point

E A Vilkov[1], **O A Byshevski-Konopko**[1], **D V Kalyabin**[2,3,*] ![ORCID] **and S A Nikitov**[2,4,5]

[1] Kotel'nikov Institute of Radio-Engineering and Electronics, Fryazino Branch, Russian Academy of Sciences, Vvedensky Sq. 1, Fryazino 141120, Moscow Region, Russia
[2] Kotel'nikov Institute of Radio-Engineering and Electronics, Russian Academy of Sciences, 11-7 Mokhovaya Street, Moscow 125009, Russia
[3] HSE University, Myasnitskaya street 20, Moscow 101000, Russia
[4] Moscow Institute of Physics and Technology (National Research University), 9 Institutskiy per., Dolgoprudny 141701, Moscow Region, Russia
[5] Saratov State University, 112 Bol'shaya Kazach'ya, Saratov 410012, Russia

E-mail: dmitry.kalyabin@phystech.edu

Abstract

The spectral properties of gap electroacoustic waves in a *PT*-symmetric structure of piezoelectrics of symmetry class 6 mm separated by a gap are theoretically investigated. The spectra were calculated for lead germanate (non-zero transverse piezoactivity) and barium titanate (symmetry class 4 mm—zero transverse piezoactivity). It has been established that at a certain level of losses and gain in piezoelectrics, the symmetric and antisymmetric modes intersect. The intersection point determines the singular point of the *PT*-symmetric structure. Beyond this point, there is a violation of the symmetric and antisymmetric distribution of electric fields in the gap of the slotted structure of two identical piezoelectrics, which is confirmed by the calculation of the electric field profiles. It is shown that the dependence of the amplitude on the frequency at an exceptional point has an extremely narrow resonance peak, which opens up the possibility of creating supersensitive sensors based on *PT*-symmetric physical structures.

Keywords: *PT*-symmetry, exceptional points, electroacoustic waves, gap waves, piezoelectrics, films

(Some figures may appear in colour only in the online journal)

1. Introduction

The most popular type of waves used to study and manipulate matter is electromagnetic radiation, which can change its parameters, in particular its electric polarization [1, 2]. However, the use of ultrafast optical methods is often limited by the simultaneous generation of a large number of nonequilibrium charge carriers, which, as a consequence, leads to a significant increase in material temperature. Because of this, other wave processes are being considered. Among them, the interaction of acoustic waves with electrical systems

---

* Author to whom any correspondence should be addressed.

(electroacoustic waves), in materials such as piezoelectrics and ferroelectrics, is becoming increasingly popular because of less scattering and much better prospects for downscaling. In particular, so-called straintronics is a new area of research in magnetism and electricity with promising applications [1, 3], which represents an outstanding alternative to other wave-based approaches because of the very low attenuation of acoustic waves (phonons) compared to magnons or plasmons [4, 5]. It has been shown that magnetic straintronics can realize memory blocks with switching energies below 1 fJ, which is already very close to the Landauer theoretical limit of $k_B T \ln 2$ [6, 7]. Acoustic waves are important in many applications, such as condition monitoring of structures and nondestructive testing [4], manipulation of small objects [8, 9], or in microelectromechanical systems [10, 11].

The energy of the collective modes of electroacoustic waves can be transferred between coupled piezoelectric waveguides [10, 11]. Consequently, it is possible to influence acoustic wave propagation by changing the intrinsic attenuation in the waveguides. A particular case, when the intrinsic attenuation in one waveguide is compensated by anti-damping in the other (balanced electroacoustic losses and gain), is a system with parity-time (*PT*) symmetry. The concept of *PT* symmetry appeared in 1998 [12]. Initially it concerned quantum systems with a non-Hermitian Hamiltonian, which, however, can have a real set of eigenstates with real eigenvalues. The *PT*-symmetric Hamiltonian commutes with the parity operator $\hat{P}$ and the time reversal operator $\hat{T}$, i.e. $\hat{P}\hat{T}\hat{H} = \hat{H}\hat{P}\hat{T}$. The action of the parity operator changes the signs of the coordinate **r** and momentum **p**, so that $\mathbf{r} \rightarrow -\mathbf{r}$, $\mathbf{p} \rightarrow -\mathbf{p}$, while the time reversal operator leads to the following transformations $\mathbf{r} \rightarrow \mathbf{r}$, $\mathbf{p} \rightarrow -\mathbf{p}$, and also leads to the complex conjugation $i \rightarrow -i$. A system described by a Schrödinger type equation with a complex potential $U(x)$, is called *PT*-symmetric if $U(x)$ has an even real part $U'(x)$ and an odd imaginary part $iU''(x)$, i.e. $U(x) = U(-x)$ and $U''(x) = -U''(-x)$. The concept of *PT*-symmetry has aroused great interest and has been extended by appropriate analogies with various physical systems, namely in optics [13, 14] (paper [14] describe electromagnetic waves in *PT*-symmetric optical structures), electronics [15], acoustics [16, 17] and magnetism [18–21].

The spectrum of a *PT*-symmetric system is usually complex, but it becomes real if the eigenmodes are invariant to the *PT*-transformation. The transition of the system into a symmetry-breaking phase occurs at the so-called exceptional point (EP), where the eigenvalues change from real to complex [22]. When the EP is passed, the eigenmodes and eigenvalues of the system become degenerate. Thus, *PT*-symmetric systems represent an exotic class of conservative systems, which simultaneously possess properties of dissipative systems. In addition, the unique nature of the *PT*-operator spectrum allows us to observe such exciting effects as, for example, single-mode laser generation [23] and magnetic permeability control at EPs [24]. The transition from the real spectrum to the complex spectrum has been observed in different systems with equally balanced gain and loss coefficients [25, 26] (in

paper [26] were considered acoustic waves in *PT*-symmetric structures). However, in acoustics *PT*-symmetric solid-state structures have not yet been considered. Papers concerned only low-frequency acoustic systems. Therefore we are planning to fill this gap, and our work is devoted to the solution to this problem.

Planar *PT*-symmetric piezoelectric waveguides have not yet been studied; they can be simple structures consisting of two (or more) piezoelectric dielectric films obtained from the same sample (thus having identical parameters). At present, studies of the dispersion properties of gap electroacoustic waves in such structures without regard to *PT*-symmetry are focused on identifying the features associated with considering the dielectric properties of the layer material placed without acoustic contact in the gap. Along with this, the differences of piezoelectrics in terms of material parameters and crystallographic symmetry were taken into account, the influence of the transverse size of one of the piezoelectrics of the layered structure was considered, and the contribution of the delay of electric fields was estimated [10, 11]. In addition to the above aspects, the influence of the relative longitudinal displacement of 4 mm (6 mm, ∞m) class piezoelectrics separated by an extremely thin gap on the behavior of gap electroacoustic waves was discussed in [27] in connection with the requests of the rapidly developing mechatronics [28].

In this paper we consider the propagation of electroacoustic waves in a *PT*-symmetric structure with a gap formed by a pair of identical piezoelectrics of symmetry class 6 mm (4, 6, 4 mm, ∞m). In the second part of the paper the model, the initial equations and the boundary conditions are considered. The third part presents the solution of the boundary problem. The fourth part is devoted to a discussion of the numerical solution of the dispersion equation, the profiles of electric fields are given. The fifth part is the conclusion.

2. Statement of the problem

In the geometry of the problem presented in figure 1, it is assumed that both crystals belong to the symmetry class 6 mm with the same orientation of the crystallographic axes 6 perpendicular to the plane of the figure. In quantum systems, the Hamiltonian is *PT*-symmetric [14] if:

$$\hat{H}(\hat{\mathbf{p}}, \hat{\mathbf{r}}, t) = \hat{H}^*(\hat{\mathbf{p}}, -\hat{\mathbf{r}}, -t) \tag{1}$$

where $\hat{\mathbf{p}}, \hat{\mathbf{r}}, t$ are momentum, radius vector and time.

Therefore, for the Schrödinger equation:

$$\left(\frac{\partial^2}{\partial x^2} + \frac{\partial^2}{\partial y^2} \right) \Psi_k(x, y) - \frac{2m(V(x, y) - E_k)}{\hbar^2} \Psi_k(x, y) = 0. \tag{2}$$

The *PT*-symmetry condition (1) reduces to the requirement that the real part of the potential $V(x, y)$ is an even function of the coordinate and the imaginary part is an odd one:
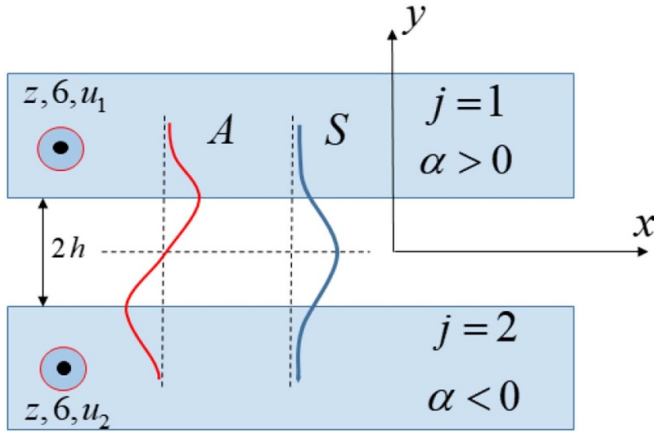
$$V(x, y) = V^*(-x, -y). \tag{3}$$

Figure 1. Scheme of the task. Letters *A*, *S* denote antisymmetric and symmetric modes.

In our case, the original equations:

$$\frac{\partial^2 u_1}{\partial t^2} = c_1^2 \nabla^2 u_1, \quad \nabla^2 \Phi_1 = 0. \tag{4}$$

The second Laplace equation (4) is *PT*-symmetric based on condition (1). The first equation (4) for a harmonic wave $u_1 \sim \exp(-i\omega t)$ has the form:

$$\left(\frac{\partial^2}{\partial x^2} + \frac{\partial^2}{\partial y^2} + \frac{\omega^2}{c_1^2} \right) u_1 = 0 \tag{5}$$

and it formally coincides with the stationary Schrödinger equation (2), if we make a formal change:

$$\begin{aligned} V(x,y) - E_k \to (\omega/c_1)^2, \quad \Psi_k(x,y) \to u_1(x,y), \\ - \hbar^2/2m \to 1. \end{aligned} \tag{6}$$

Since in quantum mechanics, the *PT*-symmetry condition for the system described by (2), reduces to the requirement imposed on the potential energy (3), then, by analogy between the potential energy in quantum mechanics and the total wave number in acoustics, the *PT*-symmetry condition for acoustic systems can be defined as a condition imposed on the total wavenumber $\Re\{k_0(\omega,x,y)\}$:

$$\Re\{k_0(\omega,x,y)\} = \Re\{k_0(\omega,-x,-y)\} \tag{7a}$$

$$\Im\{k_0(\omega,x,y)\} = -\Im\{k_0(\omega,-x,-y)\}. \tag{7b}$$

The time dependence is not included in the stationary Schrödinger equation, so the time reversal operation is equivalent to the complex conjugation operation $\hat{T}$. In what follows, by the $\hat{T}$ symmetry of a system in electroacoustics we will understand its complex conjugacy, continuing to call systems satisfying condition (7) as *PT*-symmetric.

The total wave number will be imaginary if there is either attenuation or amplification of waves in the acoustic medium.

There may be various mechanisms for such attenuation (amplification). In particular, if a piezoelectric is adjacent to a semiconductor with an electric current, then, depending on the direction of the current, the electroacoustic wave can be amplified or additionally attenuated due to the connection with the electric fields of the semiconductor. In the first stage of our research, we will not specify the type of mechanism, assuming that the total wave number is complex.

In acoustics, it is accepted that if the losses are not too large and the oscillatory process can be called quasi-periodic if an imaginary component is added to the material parameters of the composite parts. Usually, in reference data, the loss values are given in units of dB m^{-1} at a particular frequency. To convert these values into the imaginary part of the elastic modulus, one can use the following formula [29]:

$$\Im\{c_{44}\} = \frac{(\Re\{c_{44}\})^{3/2}}{20 \log e \cdot \omega^2 \sqrt{\rho}} = d \tag{8}$$

where $\Re\{c_{44}\}$ is the elasticity in the quasi-static limit, d is the decrease in the wave amplitude due to dissipation [dB m^{-1}]. Thus, the modulus of elasticity of the waves included in the velocity determines the dissipation (amplification) level, which also determines the imaginary total wave number.

In our case, the speed of shear waves of horizontal polarization in the jth piezocrystal is with elastic modulus $c_{44}^{(j)}$, piezomodulus $e_{1,5}^{(j)}$, permittivity ϵ_j and density ρ_j. Assuming the modulus to be imaginary, we, by virtue of the relation $k_0(\omega,x,y) = (\omega/c_1)$, will obtain by calculation the real and imaginary parts of the total wave number. Since we do not specify the mechanism of attenuation (amplification) of an acoustic wave, and for the sake of generality, we will choose the level of losses (amplification) in the range $\Im\{k_0(\omega,x,y)\}$ from 0 to 0.1 of $\Re\{k_0(\omega,x,y)\}$. It is easy to show that if the modulus of elasticity is imaginary $c_{44} = \Re\{c_{44}\} + i\Im\{c_{44}\}$, then in approximation $(\Im\{k_0(\omega,x,y)\})^2 \ll (\Re\{k_0(\omega,x,y)\})^2$ the following relation holds:

$$\frac{\Re\{k_0(\omega,x,y)\}}{\Im\{k_0(\omega,x,y)\}} \approx \frac{\Re\{c_{44}\} + \frac{4\pi e_{1,5}^{(j)2}}{\epsilon_j}}{\Im\{c_{44}\}} \equiv \alpha_{\text{coeff}} \tag{9}$$

where we agreed to consider the coefficient α_{coeff} from 0 to 0.1. The geometry of the problem is shown in figure 1. The direction of wave propagation in crystals occurs along the x axis (see figure 1). For the wave to increase along the propagation direction, we must assume that $\Im\{k_0\} < 0$ (upper crystal, $j = 1$), and to attenuate the wave $\Im\{k_0\} > 0$ (lower crystal, $j = 2$). Since the media differ only in the sign of the imaginary part of the total wave number, these media will be *PT*-symmetric by condition (7). We will look for the solution of equation (4) for the upper, and lower crystal, in the gap:

$$
\begin{aligned}
u_1 &= U_1 \exp(i\varphi)\exp(-s_1(y-h))\exp(\alpha x), \\
u_2 &= U_2 \exp(i\varphi)\exp(s_2(y+h))\exp(-\alpha x), \\
\Phi_1 &= F_1 \exp(i\varphi)\exp(-k(y-h))\exp(\alpha x)\exp(i\alpha(y-h)), \\
\Phi_2 &= F_2 \exp(i\varphi)\exp(k(y+h))\exp(-\alpha x)\exp(i\alpha(y+h)), \\
\Phi_0 &= \exp(i\varphi)\,[A\exp(-\alpha x)\exp(-k(y+h))\exp(-i\alpha(y+h)) \\
&\quad + B\exp(\alpha x)\exp(k(y-h))\exp(-i\alpha(y-h))] \\
\varphi &= kx - \omega t
\end{aligned}
\tag{10}
$$

where the quantities $s_{1,2}$ are defined by the equalities:

$$
\begin{aligned}
s_1 &= \left[(k-i\alpha)^2 - \left(\frac{\omega}{c_1}\right)^2\right]^{1/2}, \\
s_2 &= \left[(k+i\alpha)^2 - \left(\frac{\omega}{c_2}\right)^2\right]^{1/2}.
\end{aligned}
\tag{11}
$$

The sign of the magnitude α is the imaginary magnitude of the longitudinal propagation vector k (component along the x axis) . The sign and its value will be completely determined, according to the form of equation (5), by the imaginary part $\Im\{k_0\}$ of the total wave vector, which in turn depends on the imaginary part of the modulus of elasticity. Since the final form of the dispersion relation traditionally [30–33] includes the dependence $s_{1,2}$ on the longitudinal wave number, i.e. on the contrary, the longitudinal wave number is given first, and all other quantities are calculated through it, due to relations (8) and (11), we can supplement it with the following expression for further convenience of calculation:

$$
\frac{k}{\alpha} \approx \frac{\Re\{k_0(\omega, x, y)\}}{\Im\{k_0(\omega, x, y)\}} \approx \frac{\Re\{c_{44}\} + \frac{4\pi e_{1,5}^{(j)2}}{\epsilon_j}}{\Im\{c_{44}\}} \equiv \alpha_{\mathrm{coeff}}.
\tag{12}
$$

Thus, setting the longitudinal wave number and determining the imaginary part according to (12) and relation (7):

$$
k^{(j)} = k \pm i\alpha.
\tag{13}
$$

where the minus sign is for the upper crystal (wave amplification) $j = 1$, the plus sign is for the lower crystal (wave attenuation) $j = 2$ (see figure 1). For a given dependence of the electroacoustic wave on the x coordinate $\sim \exp(ik^{(j)}x)$, we will consider, according to the relations (7) and (13) *PT*-symmetric system from two piezoelectrics (see figure 1).

The question remains how to excite electroacoustic waves with the same amplification (attenuation) level in practice in such a structure, assuming that the film is sufficiently thick (much larger than the wavelength). One of the ways can be using semiconductors with electric current with acoustic contact with piezoelectric films [34, 35]. As a rule, the amplification effect due to the charge carrier drift current is observed in a thin boundary layer of the order of a wavelength. However, it was shown in [36] that amplified electroacoustic waves could

have the character of volume propagation. A small difference from the spectrum of electroacoustic waves at the free boundary of the piezoelectric and a small propagation angle (several degrees from the surface of the piezoelectric) can allow this wave to be excited in the gap of two piezoelectrics, either with amplification or attenuation, changing the direction of the electric current in the semiconductor. In this case, it is necessary to provide the same level of amplification and attenuation of the waves, which is usually difficult to implement in practice since the curve of the dependence of amplification on the drift velocity of charge carriers has an asymmetric shape when the sign of the velocity changes. Our preliminary calculations show that at different loss and gain levels the *PT*-symmetry can be violated. More on this will be presented in a separate future work.

In acoustoelectronics, as independent quantities that determine the state of a piezoactive medium in the ferroelectric phase, one usually chooses the elastic deformation specified by the strain tensor:

$$
u_{ik} = \frac{1}{2}\left(\frac{\partial u_i}{\partial x_k} + \frac{\partial u_k}{\partial x_i}\right)
\tag{14}
$$

and electric field E_j. If the deformation process is adiabatic, then the equations of state take the form [37]:

$$
\begin{aligned}
T_{ik} &= c_{iklm}u_{lm} - e_{j,ik}E_j, \\
D_p &= \epsilon_{pq}E_q + 4\pi e_{p,rm}u_{rm}.
\end{aligned}
\tag{15}
$$

Here T_{ik}—is the mechanical stress tensor, which, like the strain tensor u_{ik} from (14), is a symmetric tensor of the second rank; c_{iklm}, $e_{j,ik}$ and ϵ_{pq} are, respectively, the tensor of the elastic, piezoelectric and dielectric moduli of the crystal. In equation (15), where the quantity D_p is the electric induction vector, the summation is implied over repeated tensor indices. The initial equations are the crystal motion equations:

$$
\rho\frac{\partial^2 u_i}{\partial t^2} = \frac{\partial T_{ik}}{\partial x_k}
\tag{16}
$$

and Maxwell's equations in the quasi-static form:

$$
E_i = -\frac{\partial \phi}{\partial x_i}, \quad \frac{\partial D_k}{\partial x_k} = 0.
\tag{17}
$$

Here the differential operator $\partial/\partial x_i$ is considered as a vector, ϕ is the electric potential, and ρ is the density of the crystal.

For the joint consideration of equations (14)–(17), we specify the type of crystal symmetry and the geometry of acoustic wave propagation. Let us assume that a ferroelectric of class 6 mm (4, 6, 4 mm, ∞m) has a crystallographic orientation such that the sixth-order symmetry axis is parallel to the z, where z is the axis of the laboratory reference frame $x0yz$. For a given type of crystal symmetry, the initial equations (14)–(17) after some transformations can be represented as:

$$4\pi\, e_{1,5}\left(\frac{\partial^2 u_z}{\partial x^2}+\frac{\partial^2 u_z}{\partial y^2}\right)+4\pi\, e_{3,3}\frac{\partial^2 u_z}{\partial z^2}$$
$$+4\pi(e_{1,5}+e_{3,1})\frac{\partial}{\partial z}\left(\frac{\partial u_x}{\partial x}+\frac{\partial u_x}{\partial x}\right)$$
$$=\epsilon_1\left(\frac{\partial^2\phi}{\partial x^2}+\frac{\partial^2\phi}{\partial y^2}\right)+\epsilon_3\frac{\partial^2\phi}{\partial z^2} \tag{18}$$

$$\rho\frac{\partial^2 u_x}{\partial t^2}=c_{11}\frac{\partial^2 u_x}{\partial x^2}+c_{66}\frac{\partial^2 u_x}{\partial y^2}+c_{44}\frac{\partial^2 u_x}{\partial z^2}+(c_{12}+c_{66})\frac{\partial^2 u_y}{\partial x\partial y}$$
$$+(c_{13}+c_{44})\frac{\partial^2 u_z}{\partial x\partial z}+(e_{1,5}+e_{3,1})\frac{\partial^2\phi}{\partial x\partial z},$$
$$\rho\frac{\partial^2 u_y}{\partial t^2}=c_{66}\frac{\partial^2 u_y}{\partial x^2}+c_{11}\frac{\partial^2 u_y}{\partial y^2}+c_{44}\frac{\partial^2 u_y}{\partial z^2}+(c_{12}+c_{66})\frac{\partial^2 u_x}{\partial x\partial y}$$
$$+(c_{13}+c_{44})\frac{\partial^2 u_z}{\partial y\partial z}+(e_{1,5}+e_{3,1})\frac{\partial^2\phi}{\partial y\partial z},$$
$$\rho\frac{\partial^2 u_z}{\partial t^2}=c_{44}\left(\frac{\partial^2 u_z}{\partial x^2}+\frac{\partial^2 u_z}{\partial y^2}\right)+c_{33}\frac{\partial^2 u_z}{\partial z^2}+(c_{13}+c_{44})$$
$$\times\left(\frac{\partial^2 u_x}{\partial x\partial z}+\frac{\partial^2 u_y}{\partial y\partial z}\right)+e_{1,5}\left(\frac{\partial^2\phi}{\partial x^2}+\frac{\partial^2\phi}{\partial y^2}\right)+e_{3,3}\frac{\partial^2\phi}{\partial z^2}. \tag{19}$$

The resulting system of equation (19) together with equation (18) describes the dynamic behavior of a piezoelectric class 6 mm (4, 6, 4 mm, ∞m) and is often called the system of piezoacoustics equations. Let acoustic waves propagate perpendicular to the symmetry axis of a higher-order crystal. Under these conditions, the solution will not depend on the z coordinate, and the equation (19) will split into two independent systems of equations. The first one:

$$\rho\frac{\partial^2 u_x}{\partial t^2}=c_{11}\frac{\partial^2 u_x}{\partial x^2}+c_{66}\frac{\partial^2 u_x}{\partial y^2}+(c_{12}+c_{66})\frac{\partial^2 u_y}{\partial x\partial y}$$
$$\rho\frac{\partial^2 u_y}{\partial t^2}=c_{66}\frac{\partial^2 u_y}{\partial x^2}+c_{11}\frac{\partial^2 u_y}{\partial y^2}+(c_{12}+c_{66})\frac{\partial^2 u_x}{\partial x\partial y} \tag{20}$$

describes waves of vertical polarization: $\mathbf{u}\perp\mathbf{z}$. The second system, supplemented by equation (18):

$$\rho\frac{\partial^2 u_z}{\partial t^2}=c_{44}\left(\frac{\partial^2 u_z}{\partial x^2}+\frac{\partial^2 u_z}{\partial y^2}\right)+e_{1,5}\left(\frac{\partial^2\phi}{\partial x^2}+\frac{\partial^2\phi}{\partial y^2}\right)$$
$$\times 4\pi\, e_{1,5}\left(\frac{\partial^2 u_z}{\partial x^2}+\frac{\partial^2 u_z}{\partial y^2}\right)=\epsilon_1\left(\frac{\partial^2\phi}{\partial x^2}+\frac{\partial^2\phi}{\partial y^2}\right) \tag{21}$$

describes waves of horizontal polarization: $\mathbf{u}\parallel\mathbf{z}$.

Waves of horizontal and vertical polarization do not interact with each other. In this case, elastic displacements in vertical polarization waves are not coupled with an electric field, and the crystal behaves concerning them as an ordinary elastic medium without the piezoelectric effect. Due to the absence of interlayer interaction, vertically polarized waves are of no interest and are not considered further. Waves of horizontal polarization with displacements of particles along the z axis are piezoactive, and an electric field accompanies them in the plane of propagation. Equation (21) can be given the form:

$$\left[\frac{1}{c_{44}^{(j)*}}\frac{\partial^2}{\partial t^2}-\nabla^2\right]u_j=0,\quad \nabla^2\Phi_j=0. \tag{22}$$

In equation (22) $c_{44}^*=c_{44}+4\pi e_{15}^2/\epsilon_1$, $\nabla^2=\partial^2/\partial x^2+\partial^2/\partial y^2$, Φ_j is the part of the total potential ϕ_j in the crystal number j:

$$\phi_j=\Phi_j-\frac{4\pi\, e^{(j)}}{\epsilon_1}u_j \tag{23}$$

which is an electric field induced from domain walls by piezoelectric polarization charges [37].

The initial equations will be the same in the laboratory reference frame $x0yz$ for the lower ($y<-h$) crystal and for the upper ($y>h$) crystal. Taking into account the horizontal polarization of electroacoustic waves and the fact that the modules $e_{1,4}=-e_{2,5}$ added to the matrix of piezoelectric moduli for class 6 mm crystals will not change the equations of piezoacoustics (22),[6] due to the difference in the material parameters of the crystals in accordance with expressions (22) and (23), we write:

$$\frac{\partial^2 u_1}{\partial t^2}=c_1^2\nabla^2 u_1,\quad \nabla^2\Phi_1=0,\quad \phi_1=\frac{4\pi\, e_{1,5}^{(1)}}{\epsilon_1}u_1+\Phi_1,$$
$$\frac{\partial^2 u_2}{\partial t^2}=c_2^2\nabla^2 u_2,\quad \nabla^2\Phi_2=0,\quad \phi_2=\frac{4\pi\, e_{1,5}^{(1)}}{\epsilon_2}u_2+\Phi_2 \tag{24}$$

here $c_j=\left[\left(c_{44}^{(j)}+\frac{4\pi e_{1,5}^{(j)2}}{\epsilon_j}\right)\rho_j^{-1}\right]^{1/2}$ is the velocity of shear horizontal waves in the jth piezocrystal with elastic modulus c_{44}^j, piezomodulus $e_{1,5}^{(j)}$, permittivity ε_j and density ρ_j. Equation (24) should be solved together with the Laplace equation:

$$\nabla^2\Phi_0=0 \tag{25}$$

for the potential Φ_0 of the electric field arising in the gap ($|y|<h$, $2h$ is the gap thickness) between the crystals. In addition, at non-metallized crystal boundaries $y=\pm h$, the requirements for the continuity of potentials and normal components D_y of the electric induction vectors and the absence of shear stresses T_{yz} must be observed.

From the equations of the piezoelectric effect (15) in the case of shear waves with polarizations of displacements along the higher-order symmetry axis, we have the following expressions for class 6 mm crystals:

$$D_y=4\pi\left(e_{1,5}\frac{\partial u}{\partial y}-e_{1,4}\frac{\partial u}{\partial x}\right)-\epsilon\frac{\partial\phi}{\partial y},$$
$$T_{yz}=c_{44}\frac{\partial u}{\partial y}+\left(e_{1,5}\frac{\partial\phi}{\partial y}+e_{1,4}\frac{\partial\phi}{\partial x}\right). \tag{26}$$

---

[6] Piezoelectric moduli correspond to additional terms in the equations of the piezoelectric effect (15) and, finally, will be reflected in the form of shear stresses and normal components of electric induction included in the boundary conditions.

They do not contain time derivatives and therefore are valid in any inertial reference frame. Consequently, they are suitable for representing the normal components of electric induction and shear stress in the laboratory reference frame for both crystals. Note that the second terms in parentheses in expressions (26) represent the piezoelectric contribution, which is specific for class 6 mm crystals, the so-called—'transverse piezoelectric effect' [30], which is usually weakly expressed. For this reason, it is sometimes neglected [31] without making a particular explanation.

Expressions (26), are necessary for the formulation of the boundary conditions. To rewrite them, we use the last of equalities (24). After simple transformations, we get:

$$D_y = -4\pi e_{1,4}\frac{\partial u}{\partial x} - \epsilon\frac{\partial \Phi}{\partial y},$$
$$T_{yz} = c_{44}^*\frac{\partial u}{\partial y} + \frac{4\pi e_{1,4}e_{1,5}}{\epsilon}\frac{\partial u}{\partial x} + \left(e_{1,5}\frac{\partial \Phi}{\partial y} + e_{1,4}\frac{\partial \Phi}{\partial x}\right). \quad (27)$$

Now, taking into account equalities (27), where it will already be necessary to index the parameters and fields with the number $j = 1, 2$, the above-mentioned boundary conditions can be written as follows:

$$\left(\frac{4\pi e_{1,5}^{(j)}}{\epsilon_j}u_j + \Phi_j\right)\bigg|_{y=(-1)^{j+1}h} = \Phi_0\bigg|_{y=(-1)^{j+1}h},$$
$$\left(4\pi e_{1,4}^{(j)}\frac{\partial u_j}{\partial x} + \epsilon_j\frac{\partial \Phi_j}{\partial y}\right)\bigg|_{y=(-1)^{j+1}h} = \frac{\partial \Phi_0}{\partial y}\bigg|_{y=(-1)^{j+1}h}. \quad (28)$$

In expressions (28), as in the previous sections, piezoelectrically hardened shear moduli of crystals are marked with an upper asterisk: $c_{44}^{(j)*} = c_{44}^{(j)} + \frac{4\pi e_{1,5}^{(j)2}}{\epsilon_j}$.

3. Dispersion relation

The solution of equation (24) is sought in the form of waves propagating along the boundaries of the structure $y = \pm h$. Because of this, we assume that u_j, Φ_j and $\Phi_0 \sim \exp[ik^{(j)}x - i\omega t]$, where $k^{(j)}$ is the wave number determined by expression (13), ω is the cyclic frequency of the gap electroacoustic wave in the laboratory reference frame. It can be seen that the replacement (13) leads to the appearance of a wave 'addition' in the fields, which is directed from the medium with attenuation ($j = 2$) to the medium with amplification ($j = 1$).

To obtain rigorous dispersion relation we need to match wave profiles from (10) at structure boundaries $y = \pm h$ (see figure 1). The complete derivation of the boundary conditions is too complicated and is given in appendix. In the absence of damping and amplification, the dispersion equation (A.5) has the form:

$$\left[(K^2 - \epsilon K_\perp^2) - (1+\epsilon)\frac{s}{k}\right] = \pm e^{-2\xi}\left[(K^2 + \epsilon K_\perp^2) - (1-\epsilon)\frac{s}{k}\right] \quad (29)$$

where the quantities $K_\perp^2 = 4\pi e_{1,4}^2/(c_{44}^*\epsilon)$ and $K^2 = 4\pi e_{1,5}^2/(c_{44}^*\epsilon)$, are the squares of the coefficients of the electromechanical coupling of crystals for the transverse and longitudinal piezoelectric effects, respectively, $\exp(\xi) = \exp(kh)$. Hence we get the possibility to express s explicitly:

$$s = k\frac{(K^2 - \epsilon K_\perp^2) \mp (K^2 + \epsilon K_\perp^2)e^{-2\xi}}{(1+\epsilon) \pm (\epsilon - 1)e^{-2\xi}}. \quad (30)$$

Compared with the result in [32], formula (30) has a more straightforward form. There, hyperbolic functions were used instead of exponentials, but apparently, a mistake was made when writing s. The correct representations of the roots, as it is easy to show based on (30), are as follows:

$$s_+ = k\frac{K^2 - \epsilon K_\perp^2\,\mathrm{cth}(\xi)}{1 + \epsilon\,\mathrm{cth}(\xi)}, \quad s_- = k\frac{K^2\mathrm{cth}(\xi) - \epsilon K_\perp^2}{\mathrm{cth}(\xi) + \epsilon}. \quad (31)$$

In the particular case of piezoelectrics of the 6 mm class, when there is no transverse piezoactivity of the crystals ($K_\perp = 0$), expressions (31) turn, as expected, into the formulas of [34].

In our case, as well as for optical systems, *PT*-symmetry condition can be satisfied only for a discrete frequency set. However, in the specific physical structure with fixed geometrical and material parameters discrete set of frequencies is strictly equal to a particular set of wavenumbers. In magnonics wave properties can be easily tuned by changing the saturation magnetic field. And frequency representation can be more useful (see our recent paper [20]). Here we follow wavenumber representation that is common in acoustoelectronics. An essential advantage of the explicit representation of the spectrum of gap electroacoustic waves by formulas (30) and (31) is the fact that when establishing their general dispersion properties, there is no need to solve transcendental equations numerically. Thus, having determined by a simple calculation s for a chosen value of k, and then using formulas (11) one can always set the value ω corresponding to this k (and this s), and then find the phase velocity of the wave. Another advantage of formulas (30) and (31) is the explicit separation of the spectrum into modes—symmetric (upper signs in (30) and s_+ in (31)) and antisymmetric (lower signs in (30) and s_- in (31)), named following the nature of the distribution of the electric potential across the gap [32, 33]. The general picture of the mode spectra of gap electroacoustic waves for identical hexagonal crystals without damping and amplification is shown in figure 2.

The spectra of the symmetric and antisymmetric modes of the gap electroacoustic waves are marked in figure 2 with plus and minus signs, respectively. Dashed straight lines *I* and *II* depict the linear spectra of an electroacoustic waves on the metallized $s = kK^2$ and non-metallized $s = k(K^2 - \epsilon K_\perp^2)/(1 + \epsilon)$ boundaries of a piezoelectric crystal [28]. As for the point of origin of the symmetric mode $\xi^* = (kh)^*$, then, according to the first of expressions (31), it is easily established by the condition $s_+ = 0$ by the equality:

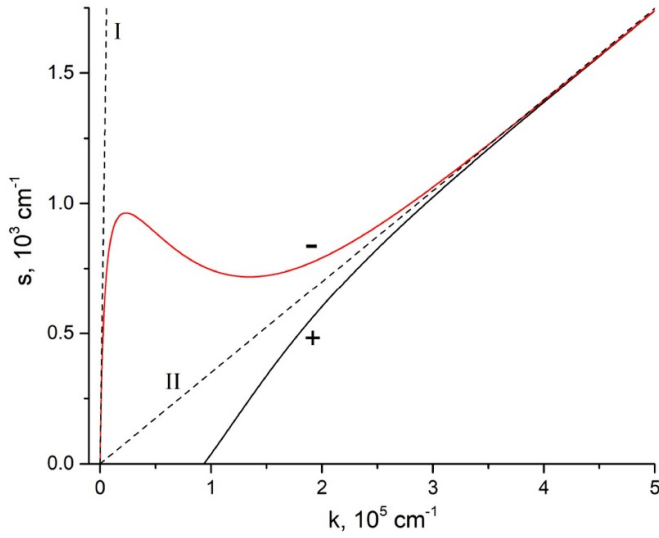$$\xi^* = \mathrm{artanh}\left(\xi\frac{K_\perp^2}{K^2}\right). \quad (32)$$

Figure 2. Mode spectrum of gap electroacoustic waves with lead germanate (Pb$_5$Ge$_3$O$_{11}$, class 6 mm) parameters. (+) sign corresponds to symmetric mode, (−) sign—antisymmetric.

(a)

(b)

(c)

Figure 3. Spectra of gap electroacoustic waves.

Expression (32) shows that the relative contribution of the transverse piezoelectric effect to the total piezoelectric activity of the crystal determines the value of ξ^*. For piezoelectrics of class 6 mm (4 mm, ∞m) there is no transverse piezoactivity and, therefore, $\xi^* = 0$, which ensures the existence of a symmetric mode on par with an antisymmetric one in the entire spectral range. On the contrary, for class 622 (422), piezoelectrics, which have only transverse piezoactivity, equality (32) ($K^2 = 0$) is also not realized, but already because of the negative coefficient of the boundary oscillation localization: $s_- < 0$.

For crystals with mixed-type piezoactivity, along with the condition $\xi > \xi^*$ for the symmetric mode, it is necessary, generally speaking, to consider the condition for the existence of the antisymmetric mode $s_- \geqslant 0$. The equal sign here corresponds to the point ξ^{**}, defined by a formula of the form (32), but with an inverted argument for the function of the hyperbolic arc tangent. However, for admissible values of ξ: $1 \leqslant \tanh(\xi) \leqslant K^2/(\epsilon K_\perp^2$, the restriction $\xi \leqslant \xi^{**}$ is equivalent to the requirement $\xi < \infty$ ($\xi^{**} \to \infty$), so that the qualitative picture of the spectrum in figure 2 will remain unchanged. The only caveat will be that with an increase in the transverse piezoactivity of the crystal against the background of its predominant longitudinal piezoactivity, asymptote *II* has a greater slope, merging with the horizontal axis in the limit of balanced piezoactivity $\epsilon K_\perp^2 \to K^2$. According to (32) $\xi^* \to \infty$, i.e. symmetric mode does not exist in the latter case.

4. Results and discussion

Figure 3(a) (Pb$_5$Ge$_3$O$_{11}$) and (b) (BaTiO$_3$) show the numerical calculation of the dispersion equation (A.5) for various values of the coefficient α_{coeff}. The first material, the spectrum of which is shown in figure 3(a), is lead germanate
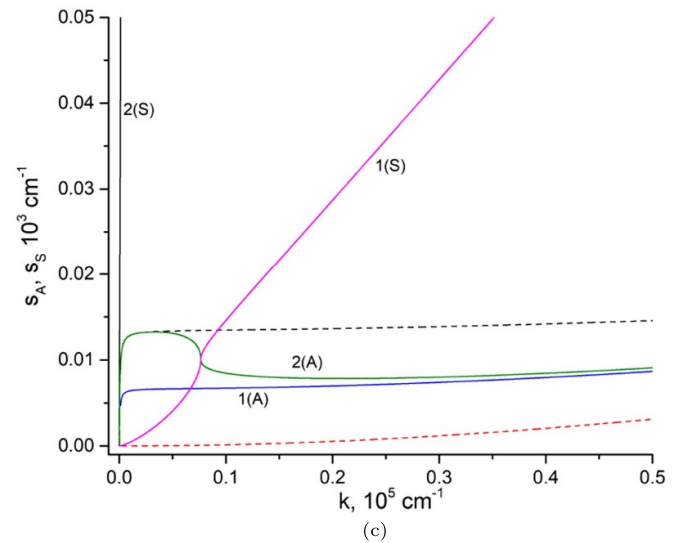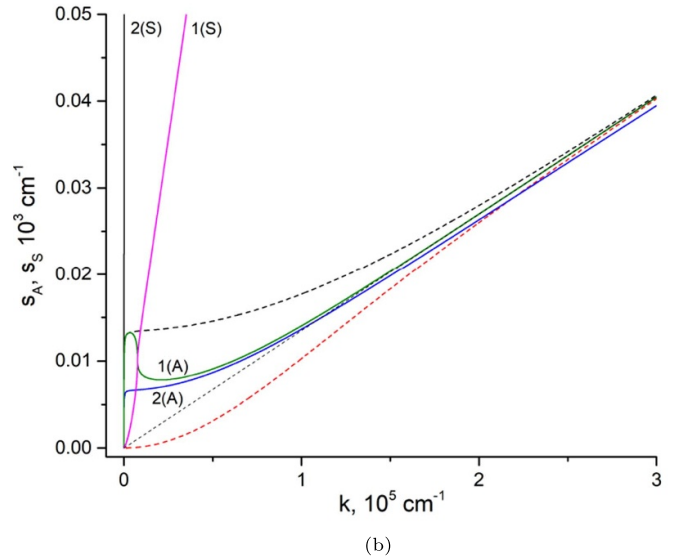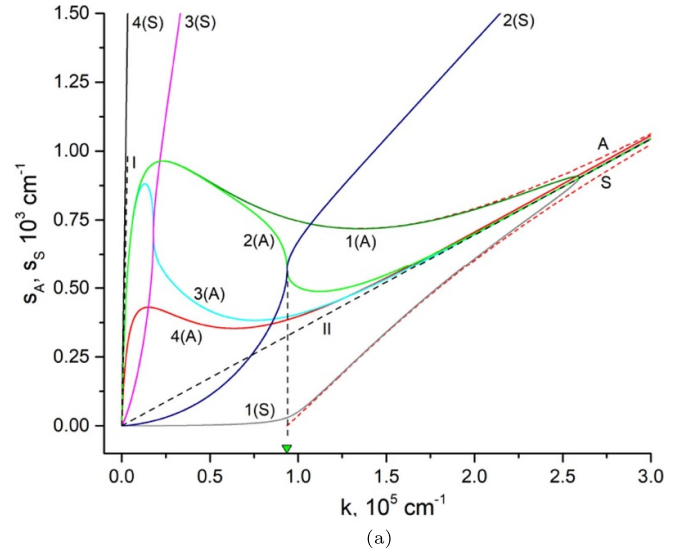
Pb$_5$Ge$_3$O$_{11}$ of symmetry class 6 mm (non-zero transverse piezoactivity) with parameters: $K^2 = 0.3, K_\perp^2 = 0.001, \epsilon = 22$ [38]. In calculating the spectrum for this material, for reasons

of clarity, we used the value of the parameter $K_\perp^2 = 0.01$, which is ten times greater than the tabulated value. On the whole, this replacement slightly changes the form of the spectrum, but in this case, we can distinguish the point of origin of the symmetric mode from zero on the wavenumber axis. Figure 3(b) shows the spectrum for the second material, BaTiO$_3$ of the 4 mm symmetry class with the parameters: $K^2 = 0.27, K_\perp^2 = 0, \epsilon = 2000$ [38]. Figure 3(c) shows a spectrum fragment in figure 3(b) in the region of small wavenumbers. Thin dashed curves *I* and *II* represent the mode spectrum of gap electroacoustic waves without attenuation and amplification (see figure 2). They in figure 3(a) almost coincide with the curves. Dashed curves *S* and *A* (symmetric and antisymmetric modes) represent the spectrum of gap electroacoustic waves without attenuation and amplification. It should be noted here that *s* quantities depend on $\xi = k \cdot h$ variable (see equation (31)). Due to this fact mode spectrum is not changed qualitatively by changing *h* parameter. It is just scaled inversely proportional to *h*.

It can be seen that considering damping and amplification in neighboring piezoelectrics leads to the fact that the larger the value of α_{coeff}, the steeper the curve of the 'symmetric' mode becomes. The curves of the 'symmetric and antisymmetric' modes move towards each other so that at specific values α_{coeff} (at $\alpha_{coeff} > 10^{-6}$) they intersect. At $\alpha_{coeff} > 10^{-3}$ the curve of the symmetric mode becomes straight and already lies higher in the values s_1 of the curve of the 'antisymmetric' mode. It can be assumed that beyond the point of intersection of the modes of the gap structure, by analogy with optical and magnetic systems [14], there is a violation of the purely symmetric (antisymmetric) distribution of fields over the thickness of the structure. The intersection point has received the name in the literature of an EP, which has several interesting properties for *PT*-symmetric structures. An essential characteristic of EPs is that not only eigenvalues degenerate at them but also the corresponding eigenvectors [12]. In Hermitian systems, the eigenvalue space has a double cone topology with degeneracy points at the vertices of the cones. In contrast, in non-Hermitian systems, the eigenvalue space is a Riemannian sheet centered near the EPs [26]. This unique characteristic makes it possible to create ultrasensitive sensors based on *PT*-symmetric physical structures [39]. These structures, indeed, have a strikingly narrow resonance curve. At the end of the article, we will demonstrate this by calculating the dependence of the amplitude on the frequency.

According to figure 3, one can go to the EP by selecting the appropriate wavenumber or increasing the amplification (attenuation) level. When $\alpha_{coeff} < \alpha_{coeff}^P$, consideration of the amplification and attenuation, leads to the symmetricity of the profile, while at $\alpha_{coeff} > \alpha_{coeff}^P$ the symmetric mode disappears completely, degenerating into a quasi-antisymmetric mode. Such a threshold behavior of the symmetry of wave fields depending on the level of losses (gain) is typical for *PT*-symmetric systems [14]. It can be seen from figure 3(a) that if we fix the wavenumber at the level of the EP for $\alpha_{coeff} = 2.12 \cdot$
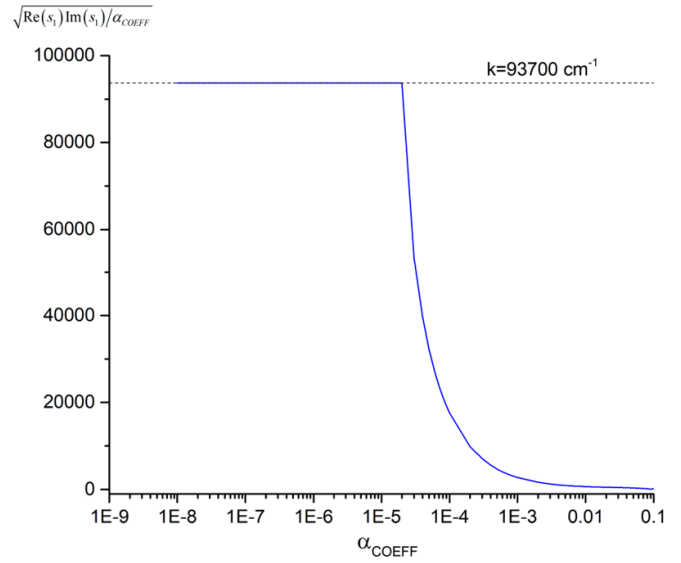

Figure 4. $\sqrt{\Re\{s_1\}\Im\{s_1\}/\alpha_{coeff}}$ dependence on α_{coeff}. It can be seen that if $\alpha_{coeff} \ll \alpha_{coeff}^p$' ($\alpha_{coeff}^p \approx 2.1 \cdot 10^{-5}$) then $k \approx 9.36 \cdot 10^4$ cm^{-1} and decreases abruptly with $\alpha_{coeff} > \alpha_{coeff}$.

10^{-5}, which is equal to $k = 93600$ and denoted by a triangle on the axis of the wavenumbers, then as we increase α_{coeff} from zero to a value greater than $\alpha_{coeff} = 2.12 \cdot 10^{-5}$ we get a threshold symmetry breaking at the point $\alpha_{coeff} = 2.12 \cdot 10^{-5}$. This assumption must be confirmed by calculating the mode field profile.

To build the dependencies of the total potential (the sum of the elastic and electric parts):

$$\varphi_1 = (gKu_1 + \Phi_1)\Big|_{y<h}, \quad \varphi_2 = (gKu_2 + \Phi_2)\Big|_{-h<y},$$
$$\varphi_0 = \Phi_0\Big|_{-h<y<h} \tag{33}$$

on the coordinate *y*, taking into account expressions (10), it is necessary to find the condition under which the 'symmetric' mode becomes completely symmetric. Based on the type of solutions (10) we can assume that this point corresponds to the condition of *PT*-symmetry of the solution for the shear displacement, i.e.:

$$\Re\{s_1\} = \Re\{s_2\}, \quad \Im\{s_1\} = -\Im\{s_2\} \tag{34}$$

where $\Re\{\}$ and $\Im\{\}$ correspond to real and imaginary parts.

From relation (11) we find:

$$k - \sqrt{\frac{\Re\{s_1\}\Im\{s_1\}}{\alpha_{coeff}}} = 0. \tag{35}$$

Figure 4 shows the dependence of the second part of the expression (35) for a fixed wavenumber (shown in figure 3 by a green triangle).

It can be seen that at $\alpha_{coeff} < \alpha_{coeff}^P$ ($\alpha_{coeff}^P \approx 2.1 \cdot 10^{-5}$) expression (35) is equal to zero and increases abruptly at

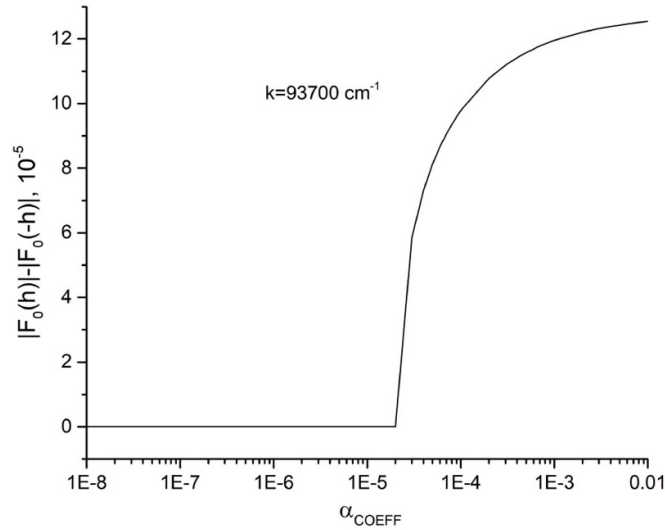**Figure 5.** Dependence of amplitude difference of electric potential on the gap boundaries $|\Phi_0(h) - \Phi_0(-h)|$ (see (10)) on α_{coeff}.
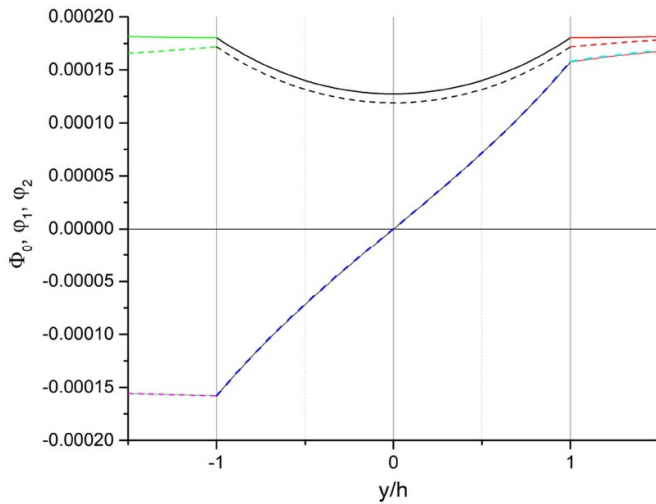

Figure 6. Total potential profile (33) for symmetric and antisymmetric modes at $\alpha_{\text{coeff}} = 10^{-6}$ for the wave vector $k = 93\,600\,\text{cm}^{-1}$. The dashed curves are the mode profile for $\alpha_{\text{coeff}} = 0$.
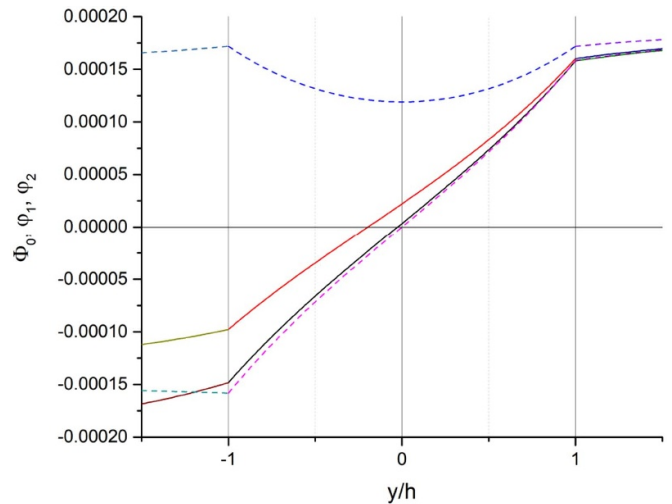

Figure 7. Total potential profile (33) for symmetric and antisymmetric modes at $\alpha_{\text{coeff}} = 10^{-4}$ for the wave vector $k = 93\,600\,\text{cm}^{-1}$. The dashed curves are the mode profile for $\alpha_{\text{coeff}} = 0$.

$\alpha_{\text{coeff}} > \alpha_{\text{coeff}}^P$. Thus, one can indirectly observe the threshold disappearance of the symmetry of the distribution of fields due to the difference in the coefficients of boundary localization since condition (34) is not satisfied. The threshold behavior of the spectral characteristics on the magnitude of losses and amplification is also confirmed by the calculation of the difference in the amplitudes of the electric potential in the gap Φ_0 at $y = \pm h$, which is shown in figure 5. At $\alpha_{\text{coeff}} < \alpha_{\text{coeff}}^P$ this difference is zero, and at $\alpha_{\text{coeff}} > \alpha_{\text{coeff}}^P$ it increases abruptly.

Figures 6 and 7 shows the profiles of the fields of the total potential (33) at the point $k = 93\,600\,\text{cm}^{-1}$ (shown in figure 3 by a green triangle) for the 'symmetric' mode and the antisymmetric mode at $x = 0$. The calculation taking into account the dependence of the amplitudes on the coordinate x, must be accompanied by the calculation of the

acoustic Poynting vector since the fields (A.1) have wave components of the type $\exp(\pm i\alpha y)$. This will allow us to calculate the total energy flow, considering all the field components. The dashed curves are the field profile for $\alpha_{\text{coeff}} = 10^{-4}$. It can be seen that at $\alpha_{\text{coeff}} < \alpha_{\text{coeff}}^P$ the field profile of the electroacoustic wave is symmetric, while at $\alpha_{\text{coeff}} > \alpha_{\text{coeff}}^P$ the field symmetry is violated. Thus, our assumption about the threshold behavior of the symmetric mode profile distribution is clearly confirmed by calculations. As shown in [25], with increasing losses, the energy flow becomes asymmetric, and the propagation of waves occurs predominantly in one of the media.

Figures 8(a) and (b) shows the dependence of the amplitude of the electric potential of the symmetric mode at $y = 0$ (middle of the gap) on the wave number and frequency for $\alpha_{\text{coeff}} = 2.12 \cdot 10^{-5}$. As expected at the EP $k = 93\,600\,\text{cm}^{-1}$ ($\nu_R = 4.47$
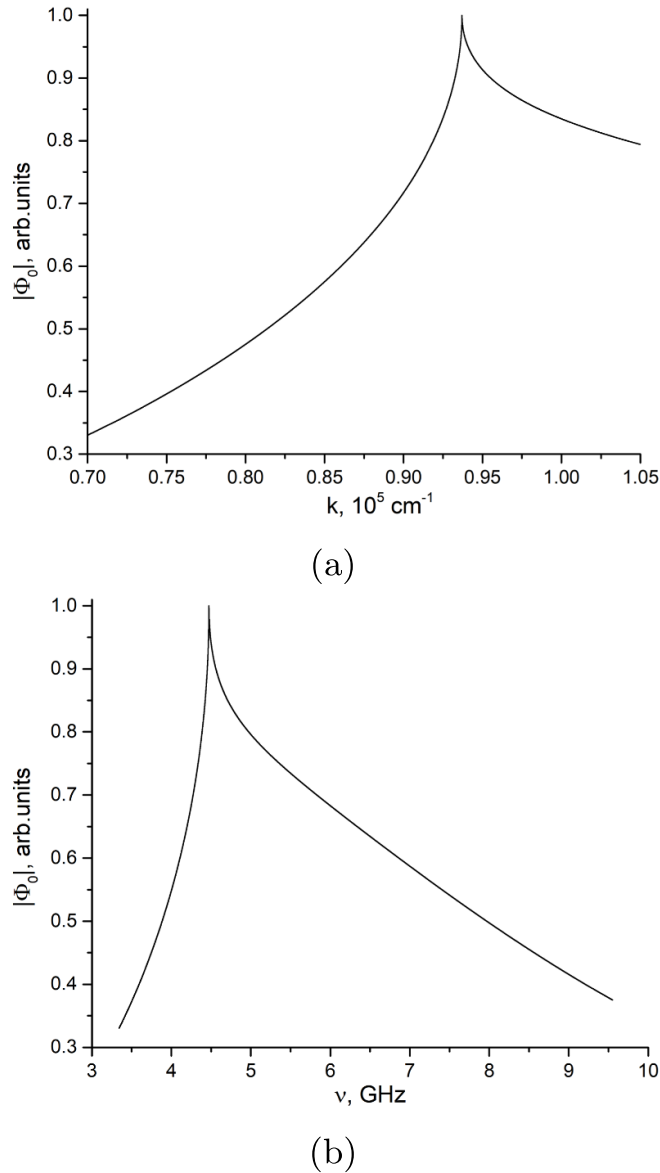
Figure 8. Dependence of the amplitude of the electric potential of the symmetric mode at $y = 0$ (the middle of the gap) for $\alpha_{\text{coeff}} = 2.12 \cdot 10^{-5}$ on (a) wavenumber and (b) frequency.

GHz). This dependence has a narrow resonance peak. The resonant linewidth of a *PT*-symmetric structure is approximately 0.33 the resonant frequency of $\nu_R = 4.47$ GHz. As mentioned earlier, this characteristic of singular points allows the creation of ultrasensitive sensors based on *PT*-symmetric physical structures [39].

5. Conclusion

The present work theoretically investigates the spectral properties of electroacoustic waves in a *PT*-symmetric structure of piezoelectrics of symmetry class 6 mm separated by a gap. The spectra (dependence of the boundary localization coefficient on the wave number) are calculated for

lead germanate (symmetry class 6 mm—non-zero transverse piezoactivity) and barium titanate (symmetry class 4 mm- zero transverse piezoactivity). It has been established that the symmetric and antisymmetric modes intersect for a particular wavenumber and at a certain level of losses and gain in piezoelectrics. The intersection point determines the EP of the *PT*-symmetric structure. Beyond this point, there is a violation of the symmetric and antisymmetric distribution of electric fields in the gap between of two identical piezoelectrics. This is confirmed by the calculation of the electric field profiles of the gap structure modes. Furthermore, it is shown that the dependence of the amplitude on the frequency at an EP has an extremely narrow resonance peak, which opens up the possibility of creating supersensitive sensors based on *PT*-symmetric physical structures.

Data availability statement

The data cannot be made publicly available upon publication because they are not available in a format that is sufficiently accessible or reusable by other researchers. The data that support the findings of this study are available upon reasonable request from the authors.

Acknowledgments

Appendix. Boundary conditions

We assume that the material parameters of the media are equal. This is one of the conditions for the *PT*-symmetry of media. Substitution of expressions (10) into boundary conditions (28) leads to the following system of six homogeneous algebraic equations for the amplitudes $U_{1,2}$, $F_{1,2}$, A and B:

$$gKU_1 + F_1 = A\exp(-2\alpha x - 2kh - 2i\alpha h) + B,$$
$$gKU_2 + F_2 = Ae^{-\xi} + B\exp(2\alpha x - 2kh + 2i\alpha h),$$
$$gK_\perp(i + \alpha/k)U_1 + \epsilon(-1 + i\alpha/k)F_1 = (-i\alpha/k + 1)$$
$$\times A\exp(-2\alpha x - 2kh - 2i\alpha h) + B(-i\alpha/k + 1),$$
$$gK_\perp(i - \alpha k)U - 2 + \epsilon(1 + \alpha k)F_1 = (-i\alpha/k - 1)A$$
$$+ B(-i\alpha/k + 1)\exp(2\alpha x - 2kh + 2i\alpha h),$$
$$g(KK_\perp(ik + \alpha) - s_1)U_1 + ((ik + \alpha)K_\perp$$
$$+ (-k + i\alpha)K)F_1 = 0,$$
$$g(KK_\perp(ik - \alpha) + s_2)U_2$$
$$+ ((ik - \alpha)K_\perp + (k + i\alpha)K)F_2 = 0. \quad (A.1)$$

Here, the quantities $K_\perp^2 = 4\pi e_{1,4}^2/(c_{44}^*\epsilon)$ and $K^2 = 4\pi e_{1,5}^2/(c_{44}^*\epsilon)$, are the squares of the coefficients of the electromechanical coupling of crystals for the transverse and longitudinal piezoelectric effects, respectively, $g = (4\pi c_{44}^{(1)*}/\epsilon)^{1/2}$, ϵ is the permittivity.

To find the dispersion equation describing electroacoustic waves in a *PT*-symmetric gap structure, we introduce the relation:

$$\alpha = \alpha_{\text{coeff}}k \quad (A.2)$$

where $\alpha_{\text{coeff}} = \alpha/k \ll 1$. According to this replacement and equations in section 2 we can obtain the following substitutes for the quantities included in the dispersion equation (A.1):

$$c_{44}^* = c_{44}^*(1 \pm \alpha_{\text{coeff}}),\ K^2 \to K^2(1 \mp \alpha_{\text{coeff}}),$$
$$K_\perp \to K_\perp^2(1 \mp \alpha_{\text{coeff}}),\ g = g(1 \pm \alpha_{\text{coeff}})^{1/2}. \quad (A.3)$$

The upper sign is for a medium with amplification and the lower one with attenuation.

A solvability requirement, expressed by the equality to zero of the determinant of the system of equation (A.1), gives the desired dispersion relation for gap electroacoustic waves in a layered structure of class 6 mm piezoelectrics with a vacuum gap. The determinant of the system of equations has the form taking into account that $\alpha_{\text{coeff}}^2 = (\alpha/k)^2 \ll 1$:

$$(1 + i\alpha_{\text{coeff}})^{3/2}k(K + iK_\perp)\Big[i(1 - i\alpha_{\text{coeff}})^{3/2}k(-K + iK_\perp)$$
$$\times \{(E\exp(4hk) - 1)(K^2 - 4\alpha_{\text{coeff}}\epsilon KK_\perp + \epsilon K_\perp^2\}$$
$$+ (1 + i\alpha_{\text{coeff}})^{1/2}((i + \alpha_{\text{coeff}})^2 kKK_\perp - is_1)$$
$$\times \{iE\exp(4hk)(\epsilon + 1)(K + i\epsilon K_\perp)$$
$$+ (K(1 - i\alpha_{\text{coeff}} - i\epsilon K_\perp(1 + i\alpha_{\text{coeff}}))(-i + \alpha_{\text{coeff}}$$
$$+ \epsilon(i + \alpha_{\text{coeff}}))\}] + (1 - i\alpha_{\text{coeff}})^{1/2}(-ik(-i + \alpha_{\text{coeff}})^2 KK_\perp + s_2)$$
$$\times \Big[(1 - i\alpha_{\text{coeff}})^{3/2}k(K - iK_\perp)\{\exp(4hk)(\epsilon + 1)(K - i\epsilon K_\perp)$$
$$+ (-1 + \epsilon + i\alpha_{\text{coeff}}(1 + \epsilon) + i\epsilon K_\perp(1 - i\alpha_{\text{coeff}}))\}$$
$$+ (1 - i\alpha_{\text{coeff}}^{1/2}\{-(-1 + \epsilon)^2 + \exp(4hk)(1 + \epsilon)^2$$
$$+ \alpha_{\text{coeff}}^2)(\exp(4hk) - 1)((1 + \epsilon)^2(-ik(i + \alpha_{\text{coeff}})^2 KK_\perp - s_1))\}\Big] = 0. \quad (A.4)$$

To calculate the field profile, we solve five equations of the system (A.1). The results of solving this system are:

$$F_1 = -g\frac{(-iKK_\perp\alpha - KK_\perp k + is_1^*)}{(K - iK_\perp)(ik + \alpha)}U_1,$$
$$A = g\frac{((-i\alpha + k)(K^2 - \epsilon K_\perp^2) - (1 + \epsilon)s_1^*)}{2k(K - iK_\perp)}\exp[2(i\alpha + k)h + 2\alpha x]U_1,$$
$$B = ig\frac{((\alpha^2 + k^2)K^2 - \epsilon(\alpha + ik)^2 K_\perp^2) + [-i\alpha(1 + \epsilon) - (\epsilon - 1)k]s_1^*)}{2k(\alpha + ik)(K - iK_\perp)}U_1,$$
$$F_2 = g(-i\epsilon k\cosh(2hk)\{\alpha^2 KK_\perp(K - iK_\perp) + k(K + iK_\perp)(kKK_\perp + is_1^*)$$
$$+ \alpha(kKK_\perp^2 + (K - iK_\perp)s_1^*)\} + \sinh(2hk)\{(\alpha + ik)^2(i\alpha + k)K^3 -$$
$$- \alpha\epsilon(\alpha^2 + k^2)K^2 K_\perp - i\alpha\epsilon(\alpha + ik)^2 KK_\perp^2 + \epsilon^2(\alpha - ik)(\alpha + ik)^2 K_\perp^3$$
$$\times s_1^*(\alpha k\epsilon(iK + K_\perp) + \alpha^2(\epsilon + 1)(K + i\epsilon K_\perp) + k^2(K + i\epsilon^2 K_\perp))\})$$
$$\times \exp[2i\alpha h + 2\alpha x](\epsilon k(\alpha^2 + k^2)(K - iK_\perp)^2)^{-1}U_1,$$
$$U_2 = (-\epsilon\exp(2hk)(\alpha^2 + k^2)i(\alpha + ik)(K^2 - \epsilon K_\perp^2) + s_1^*(1 + \epsilon)$$
$$+ (i\alpha(1 + \epsilon) + k(\epsilon - 1))\{(\alpha^2 + k^2)K^2 - \epsilon(\alpha + ik)^2 K_\perp^2$$
$$+ s_1^*(-i\alpha(1 + \epsilon) + k(\epsilon - 1))\})\exp[2i\alpha h - 2hk + 2\alpha x](2\epsilon k(\alpha^2 + k^2)$$
$$\times (K - iK_\perp)^2)^{-1}U_1. \quad (A.5)$$

where $s_1^* = s_1(1 + i\alpha_{\text{coeff}})$.

ORCID iD

D V Kalyabin https://orcid.org/0000-0001-5953-0266

References

[1] Bukharaev A A, Zvezdin A K, Pyatakov A P and Fetisov Y K 2018 *Phys.-Usp.* **61** 1175–212

[2] Atanasov V and Saxena A 2011 *J. Phys.: Condens. Matter* **23** 175301

[3] Sadovnikov A, Grachev A, Sheshukova S, Sharaevskii Y, Serdobintsev A, Mitin D and Nikitov S 2018 *Phys. Rev. Lett.* **120** 257203

[4] Caldwell J D, Lindsay L, Giannini V, Vurgaftman I, Reinecke T L, Maier S A and Glembocki O J 2015 *Nanophotonics* **4** 44–68

[5] Miao H and Li F 2021 *Ultrasonics* **114** 106355

[6] Roy K, Bandyopadhyay S and Atulasimha J 2011 *Appl. Phys. Lett.* **99** 063108

[7] Roy K 2014 *MRS Proc.* **1691** 57–62

[8] Xu D, Cai F, Chen M, Li F, Wang C, Meng L, Xu D, Wang W, Wu J and Zheng H 2019 *Ultrasonics* **93** 18–25

[9] Peng X, He W, Xin F, Genin G M and Lu T J 2020 *Ultrasonics* **108** 106205

[10] Li X-F and Yang J 2006 *Sens. Actuators* A **132** 472–9

[11] Yang J S 2005 *Math. Mech. Solids* **11** 451–8

[12] Bender C M and Boettcher S 1998 *Phys. Rev. Lett.* **80** 5243–6

[13] El-Ganainy R, Makris K G, Christodoulides D N and Musslimani Z H 2007 *Opt. Lett.* **32** 2632

[14] Zyablovsky A A, Vinogradov A P, Pukhov A A, Dorofeenko A V and Lisyansky A A 2014 *Phys.-Usp.* **57** 1063–82

[15] Schindler J, Lin Z, Lee J M, Ramezani H, Ellis F M and Kottos T 2012 *J. Phys. A: Math. Theor.* **45** 444029

[16] Fleury R, Sounas D L and Alu A 2016 *IEEE J. Sel. Top. Quantum Electron.* **22** 121–9

[17] Shi C, Dubois M, Chen Y, Cheng L, Ramezani H, Wang Y and Zhang X 2016 *Nat. Commun.* **7** 11110

[18] Galda A and Vinokur V M 2016 *Phys. Rev.* B **94** 020408(R)

[19] Liu H, Sun D, Zhang C, Groesbeck M, Mclaughlin R and Vardeny Z V 2019 *Sci. Adv.* **5**

[20] Temnaya O, Safin A, Kalyabin D and Nikitov S 2022 *Phys. Rev. Appl.* **18** 014003

[21] Sadovnikov A V, Zyablovsky A A, Dorofeenko A V and Nikitov S A 2022 *Phys. Rev. Appl.* **18** 024073

[22] Miri M-A and Alù A 2019 *Science* **363** 6422

[23] Doronin I V, Zyablovsky A A, Andrianov E S, Pukhov A A and Vinogradov A P 2019 *Phys. Rev.* A **100** 021801(R)

[24] Guang Wang X, hua Guo G and Berakdar J 2020 *Nat. Commun.* **11** 5663

[25] Guo A, Salamo G J, Duchesne D, Morandotti R, Volatier-Ravat M, Aimez V, Siviloglou G A and Christodoulides D N 2009 *Phys. Rev. Lett.* **103** 093902

[26] Yang Y, Jia H, Bi Y, Zhao H and Yang J 2019 *Phys. Rev. Appl.* **12** 034040

[27] Zelenka J 1986 *Piezoelectric Resonators and their Applications* (Elsevier)

[28] Jabłoński R, Turkowski M and Szewczyk R (eds) 2007 *Recent Advances in Mechatronics* (Springer)

[29] Auld B 1973 *Acoustic Fields and Waves in Solids* (A Wiley-Interscience publication (Wiley))

[30] Liamov V E 1983 *Polarization effects and anisotropy of the interaction of acoustic waves in crystals* (Moscow Izdatel Moskovskogo Universiteta Pt)

[31] Gulyaev Y and Plessky V 1976 *Phys. Lett.* A **56** 491–2

[32] Balakirev M K and Gilinskii I A 1977 *Phys. Solid State* **19** 613–5

[33] Gylyaev Yu V P V P 1977 *Acoust. Phys.* **23** 716–23

[34] Balakirev M K and Gilinskii I A 1982 *Waves in piezoelectric crystals* (NovosibirskIzdatel Nauka)

[35] Pustovoĭt V I 1969 *Sov. Phys. - Usp.* **12** 105–32

[36] Shevyakhov S N 1985 *Acoust. Phys.* **31** 565–7

[37] Sosnin A S and Strukov B A (eds) 1970 *Introduction to Ferroelectricity* (Vysshaya Shkola)

[38] Shaskolskaya M P (eds) 1982 *Acoustic Crystals Handbook* (Nauka)

[39] Wiersig J 2020 *Photon. Res.* **8** 1457